Lightning-generated Transients in Buildings with an Efficient PEEC Method

Ruihan Qi, Y. Du and Mingli Chen

The Hong Kong Polytechnic University, Department of Building Services Engineering, Hung Hom, Kowloon, Hong Kong

This paper presents a time-domain equivalent circuit approach for analyzing lightning-generated electromagnetic transients in modern buildings. The building is represented by a wire-plate structure, and is modeled by internal impedance and external inductance of current cells, and coefficients of potential cells. A vector-fitting technique is applied for modeling frequency-varying internal impedance for time-domain simulation. With this unique formulation, the number of unknown variables is reduced, and computational efficiency is improved significantly. Finally, lightning-generated impulse magnetic fields and voltages within a building are evaluated.

***Index Terms*— lightning; magnetic field; transient; plate; PEEC.**

I. Introduction

For safety, lightning protection systems (LPS) are provided in buildings to intercept lightning and to channel the currents to ground via down conductors. The lightning current generates substantial impulse electromagnetic (EM) transients inside buildings. These transients can cause malfunctions or damages to electronic equipment. To provide effective protection for sensitive equipment, assessment of lightning transients within buildings becomes indispensable.

Down conductors of a LPS are usually made by reinforcing bar embedded in concrete columns and beams. Note that planar structures such as metal decking and raised floor panels have been introduced in buildings for constructing composite concrete floors. These bars and plates are inter-connected to form a large wire-plate structure, as illustrated in Fig. 1. This structure can affect the lightning-generated electromagnetic environment significantly. Recently, insulated down conductors (IDCs) have been increasingly adopted for aesthetic and economic reasons. They are generally routed in electrical duct or on façade. In such cases, the wire-plate structure plays a significant role in mitigating lightning transients in buildings.

Over the years, many formulations have been developed to solve for lightning transients in wire structures, including the method of moments, finite-difference time-domain method and finite element method [1-3]. Recently both the boundary element method and finite element method have also been applied successfully to solve shielding problems in frequency domain [4-5]. These methods have great advantages in dealing complex geometry and material properties. However, there has not been any successful application in analyzing lightning transients in a complicated structure with large plates and many short wires.

The partial element equivalent circuit (PEEC) method was originally developed to model EM coupling of short wires. This technique has been recently employed to tackle magnetic field problems of plates in the frequency domain [6-7], where the plates are meshed into small volume cells with constant current density. In [8] a time-domain approach for non-linear magnetic materials was presented. In these studies a significant number of unknowns is required for modeling large plates in order to retain solution accuracy. To reduce the number of unknowns, an analytical function was introduced for current distribution across the plate thickness. This technique has been successfully applied to solve for magnetic fields [9-12] in frequency domain.

This paper presents an efficient PEEC method for analyzing time-domain lightning transients in buildings with a wire-plate structure. In Section II, circuit models for both wire and plates are presented, in which EM coupling among elements is represented with inductance and capacitance. The internal impedance and external inductance are introduced for efficient computation, and a vector fitting technique is applied for time-domain simulation. A special technique is presented to model the joint of adjacent plates. In Section III, the numerical and experimental validation of the proposed method is presented. Finally, this method is applied to evaluate lightning transients in a building.

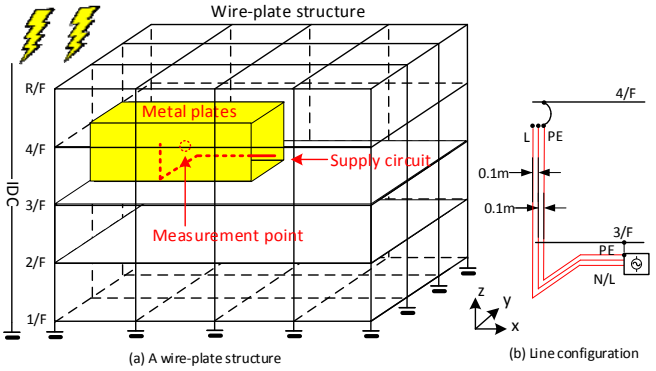

Fig. 1. Configuration of the building for transient evaluation

II. Circuit Model of Building Structures

Fig. 1 illustrates a simplified building structure for lightning analysis. It consists of a wire grid and several planar plates, which represent reinforcing bars in concrete, and metal decking or others. These metal wires and plates are bonded to the LPS, and carry the discharge current during a lightning strike.

A. Equivalent circuit

Note that the eddy current within thin plates circulates along the tangential direction. The plate with thickness *d* is divided into a number of potential cells on the *x*-*y* plane, as seen in Fig. 2. Current cells are formed by taking the volume between the

centers of adjacent potential cells. In each current cell, current density varies along its thickness, and is described by a double exponential function $J_i(z) = J_i^- e^{-\alpha z} + J_i^+ e^{\alpha z}$, $\alpha = \sqrt{j2\pi f\sigma\mu_0}$. The total cell current is obtained by integrating $J_i(z)$ over its cross section, and is equal to $I_i = (J_i^+ + J_i^+)\Delta a_i$ and $\Delta a_i = w_i \sinh(0.5\alpha d)/0.5\alpha$.

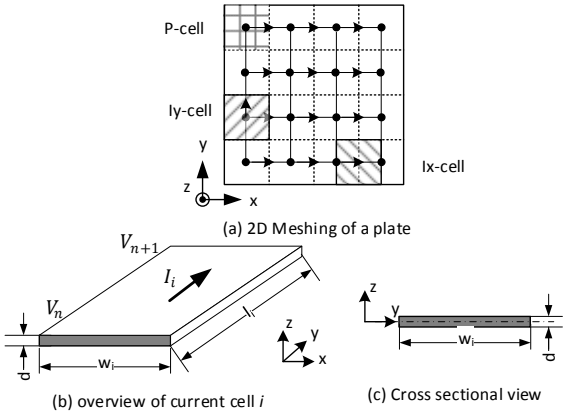

Fig. 2 Configuration of potential and current cells

It is known that electric field can be expressed using magnetic vector potential *A* and electric scalar potential *V* as,

$$\vec{E}(r) + j\omega\vec{A}(r) = -\nabla\phi(r) \tag{1}$$

With free-space Green's function $G(r,r') = 1/R$ ($R = |r - r'|$), these potentials can be expressed using J and charge density q as,

$$\begin{aligned}\vec{A}(r) &= \frac{\mu_0}{4\pi}\int G(r,r')\cdot\vec{J}(r')dv' \\ \phi(r) &= \left[4\pi\varepsilon_0\right]^{-1}\int G(r,r')\cdot q(r')ds'\end{aligned} \tag{2}$$

Integrating (1) over all four surfaces of current cell *i* yields average potential difference $V_{ij} = V_{n,j} - V_{n+1,j}$,

$$V_{ij} = \int_{S_i}\sigma^{-1}J_i ds + j\omega\int_{S_i}\int_{V_j}\left[J_j^+ e^{\alpha z'} + J_j^- e^{-\alpha z'}\right]\cdot R^{-1}dsdv' \tag{3}$$

The part contributed by E_i can be rewritten as

$$V_{ii,R} = \frac{l_i}{\sigma(1+d/w_i)}\left[1 + \frac{\cosh(0.5\alpha d)}{w_i l_i}\right]\cdot I_i \tag{4}$$

Note that $d/w_i \ll 1$. Dividing voltage in (4) by cell current I_i yields the average surface impedance of cells, as follows:

$$Z_{ii} = \frac{l_i}{\sigma w_i d}\frac{0.5\alpha d}{\tanh(0.5\alpha d)} \approx \begin{cases} l_i\left[\sigma w_i d\right]^{-1} & \alpha d << 1 \\ l_i\left[\sigma w_i 2/\alpha\right]^{-1} & \alpha d >> 1 \end{cases} \tag{5}$$

It is equal to the DC resistance at low frequency ($\alpha d \ll 1$), and an equivalent impedance determined by skin effect depth ($2/\alpha$) at high frequency ($\alpha d \gg 1$). This is certainly considered as internal impedance of cells, similar to the one for circular wires.

Similarly, ignoring the contribution from two side surfaces of the cell, the part contributed by vector potential *A* is given by

$$\begin{aligned}V_{ij,b} &= \frac{j\omega\mu_0}{8\pi w_i}\int_{S_i}\int_{V_j}\left[J_j^+ e^{\alpha z'} + J_j^- e^{-\alpha z'}\right]\left[\frac{1}{R^+} + \frac{1}{R^-}\right]dv'ds \\ &= \frac{j\omega\mu_0}{4\pi w_i\Delta a_j}\int_{S_i}\int_{S_j}\int_{-d/2}^{d/2}\frac{e^{\alpha z'} + e^{-\alpha z'}}{R^+}dsds'dz'\cdot I_i\end{aligned} \tag{6}$$

where R^+ and R^- are respectively the distances to the upper and lower surfaces of cells, i.e.,$R^{+/-} = \sqrt{\Delta x^2 + \Delta y^2 + (z \pm 0.5d)^2}$ Inductance of current cells is then obtained as follows:

$$L_{ij} = \frac{\mu_0}{4\pi}\frac{1}{w_i\Delta a_j}\int_{S_i}\int_{S_j}\int_{-d/2}^{d/2}\frac{\cosh(\alpha u)}{R^+}dsds'du \tag{7}$$

Note that $R^+ \approx \sqrt{\Delta x^2 + \Delta x^2}$ because of thin plate thickness. Therefore, L_{ij} in (7) is approximated by

$$L_{ij} \approx \frac{\mu_0}{4\pi}\frac{1}{w_i w_j}\int_{S_i}\int_{S_j}\frac{1}{\sqrt{\Delta x^2 + \Delta y^2}}dsds' \tag{8}$$

This is the inductance resulting from surface current on the cell, and is considered as external inductance of cells.

As relaxation time of a conductor is much shorter than the time of concern in transient analysis, electric charge is situated on the conductor surface and is independent of frequency and conductivity. Similar to the procedure stated for inductance calculation, average potential arising from charge *Q* is given by

$$\phi_{nm} = \frac{1}{16\pi\varepsilon\Delta s_n\Delta s_m}\int_{S_n^+ + S_n^-}\int_{S_m^+ + S_m^-}\frac{1}{R}dsds'\cdot Q_m \tag{9}$$

where surface area $\Delta s_n = w_n l_n$, $S_n^{+/-}$ is the upper/lower surface of potential cell *n*. Coefficient of potential p is then given by

$$p_{nm} = \frac{1}{16\pi\varepsilon\Delta s_n\Delta s_m}\int_{S_n^+ + S_n^-}\int_{S_m^+ + S_m^-}\frac{1}{R}dsds' \tag{10}$$

Both the branch voltage equation of current cells and the nodal potential equation of potential cells are established, as follows:

$$\begin{aligned}V_{n+1} - V_n &= Z_{i,int}(\omega) + \sum\nolimits_j j\omega L_{ij}I_j \\ V_n &= \sum\nolimits_m p_{nm}q_m\end{aligned} \tag{11}$$

Fig. 3 shows the equivalent circuit. A full network model is built up after connecting all segments according to the cell topology.

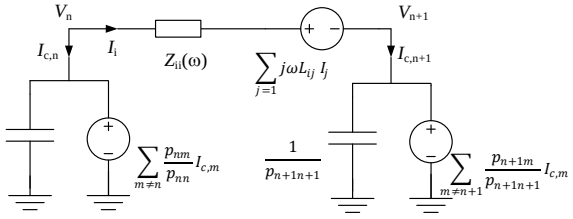

Fig. 3 Equivalent Circuit of a line segment

Circuit parameters of a circular wire of radius r_a can be obtained similarly with (1-2). They are expressed as

$$\begin{aligned}Z_{ii} &= \frac{j\omega\mu_0\Delta l_i}{2\pi\alpha r_a}\frac{I_0(\alpha r_a)}{I_1(\alpha r_a)} \\ L_{ij} &= \frac{\mu_0}{4\pi}\int_{l_i}\int_{l_j}\frac{1}{R}dl_i dl_j \\ p_{nm} &= \frac{1}{4\pi\varepsilon_0}\frac{1}{\Delta l_n\Delta l_m}\int_{l_n}\int_{l_m}\frac{1}{R}dl_n dl_m\end{aligned} \tag{12}$$

where I_k is the modified Bessel functions of the 1st kind at order *k*, and Δl_x ($x = i, j, n$ or m) is the length of wire segment *x*.

B. Technique for modelling plate joints

When two plates join together, current will flow from one plate to another. Fig. 4(a) illustrates a case of two parallel plates joined on the same plane with the *x*-dir. current flowing from one to another. To ensure the continuous current over these plates, virtual nodes are introduced at the joint of two plates. These nodes are dimensionless, and do not possess any self capacitance and mutual capacitance to other nodes. Fig. 4(b) shows the topology for a joint node. Note that the connection shown in Fig. 4(b) provides a path for the *x*-dir. current only.

C. Vector fitting method for frequency-dependent parameters

It is noted in Section II(A) that internal impedance varies with frequency significantly, while inductance and potential coefficient generally do not. To solve a frequency-variant transient problem in time domain, the vector fitting technique together with a recursive convolution technique is adopted.

Note $Z_{ii}(s)$ in s domain can be approximated with rational functions in the form of pole-residue terms as follows:

$$Z_{ii}(s) = d + sh + \sum_{m=1}^{M} \frac{r_m}{s - a_m} \tag{13}$$

where d, h, a_m and r_m are real constants. The 1st and 2nd terms are the DC resistance and inductance in the network model. The 3rd term is represented with its impulse response, as follows:

$$h(t) = \sum_{m=1}^{M} r_m e^{a_m t} \ . \tag{14}$$

With the convulsion technique the discrete voltage response $V_{fit}[n]$ given by current I is expressed by

$$\begin{aligned} V_{fit}[n] &= \sum\nolimits_{m=1}^{M} V_{fit,m}[n] \\ V_{fit,m}[n] &= R_m \cdot I[n] + K_m \cdot V_{fit,m}[n-1] \end{aligned} \ . \tag{15}$$

where $R_m = (e^{a_m T} - 1)a_m / r_m$ and $K_m = e^{a_m T}$. T is the size of time step.

D. Time-domain solution

Now the EM coupling in a wire-plate structure is represented by a mutually coupled network made with frequency-invariant components. Lightning current in the structure can be solved by a circuit analysis tool in time domain, subsequently the impulse EM field in the structure. As this formulation has fewer unknowns and frequency-independent circuit models, its computation is much faster than others.

By using the modified nodal analysis approach, a set of time-domain differential equations are obtained, as follows:

$$\begin{aligned} \mathbf{AV}(t) + \mathbf{RI}(t) + \mathbf{L}\, d\mathbf{I}(t)/dt + \mathbf{V_{fit}}(t) &= -\mathbf{A_{Vs}}\mathbf{V_s}(t) \\ \mathbf{GYV}(t) + \mathbf{F}\, d\mathbf{V}(t)/dt - \mathbf{GA}^{\mathrm{T}}\mathbf{I}(t) &= \mathbf{GA_{Is}}\mathbf{I_s}(t) \end{aligned} \ . \tag{16}$$

where $\mathbf{A}$ is the incidence matrix for the network. Both $\mathbf{A_{Is}}$ and $\mathbf{A_{Vs}}$ are respectively the incidence matrices for independent current and voltage sources. $\mathbf{Y}$ is a conductance matrix of lumped elements connected to the nodes in the network. $\mathbf{F^{-1}}$ is a matrix only retaining diagonal elements of matrix $\mathbf{P}$, and $\mathbf{G} = \mathbf{F} \cdot \mathbf{P}$. $\mathbf{V_{fit}(t)}$ is the diagonal voltage matrix determined with (13). By using the backward Eurla method, the discrete equation of (14) is obtained, as follows:

$$\begin{bmatrix} \mathbf{A} & \mathbf{R} + \sum \mathbf{R}_m + \mathbf{L}/T \\ \mathbf{GY} + \mathbf{F}/T & -\mathbf{GA}^{\mathrm{T}} \end{bmatrix} \begin{bmatrix} \mathbf{V}[n] \\ \mathbf{I}[n] \end{bmatrix} = \begin{bmatrix} \mathbf{A_{Vs}} V_s[n] \\ \mathbf{GA_{Is}} I_s[n] \end{bmatrix} + \begin{bmatrix} \mathbf{L}/T\, \mathbf{I}[n-1] + \sum \mathbf{K}_m \mathbf{V}_{fit,m}[n-1] \\ \mathbf{F}/T \mathbf{V}[n-1] \end{bmatrix} \tag{17}$$

III. Experimental and Numerical Validation

The proposed method is experimentally validated against the results obtained from the wire-plate structure shown in Fig. 5. The structure has two parallel aluminum plates of 0.4 m x 0.4 m x 1.5 mm with the spacing of 0.4 m, connected with two thin aluminum bars of 1.5 mm x 30 mm. The structure is connected to an impulse generator with ϕ1.4 mm round copper conductors.

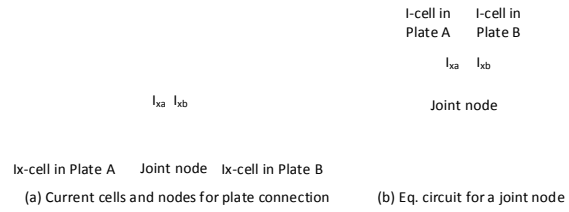

Fig. 4. Modeling of a plate joint

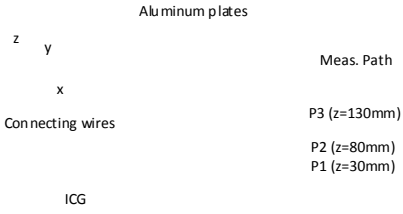

Fig. 5 Experiment setup for validating the proposed model

Both the impulse magnetic field in the structure and source current are measured with a tailor-made field probe and a Pearson current probe 4997 together with a digital oscilloscope. The field probe consists of a magneto-resistive sensor HMC1053, a low-noise broadband amplifier and a power drive circuit, as shown in Fig. 6(a). The device has a bandwidth from dc to 10MHz, and a measurement range of +/- 6 Gauss. The field probe was calibrated with impulse magnetic fields, and its sensitivity was found to be 2.3G/V.

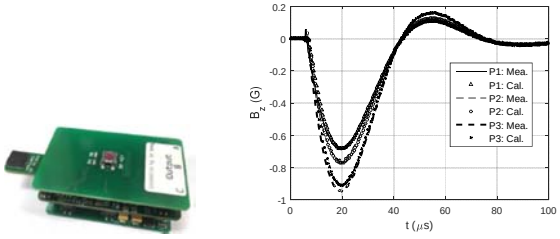

(a) Field probe (b) Magnetic field comparison

Fig. 6 Measured and calculated magnetic field within the structure

Fig. 6(b) shows both the measured and calculated magnetic field at three points along a vertical line located at the structure center, as indicated in Fig. 5. The source current has a peak value of 218A. In the calculation, each of the plates is uniformly divided into 40 x 40 cells. It is found that the matching between measured and calculated magnetic field is very good, with an error smaller than 5%.

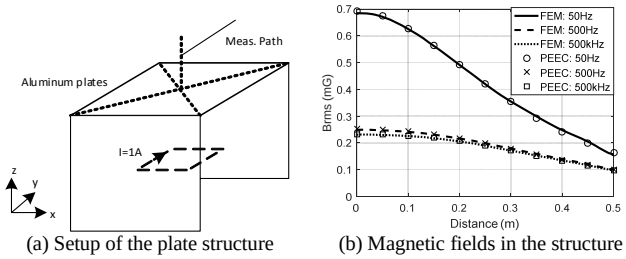

(a) Setup of the plate structure (b) Magnetic fields in the structure

Fig. 7 Numerical comparison between FEM and PEEC methods

The proposed method is validated also numerically, against the results obtained by a FEM-based software (ANSYS Maxwell) as well. Fig. 7(a) shows the configuration of the testing setup. A U-shape shield is constructed with three identical plates (0.4 m x 0.4 m x 2 mm). A loop current source

is placed at a distance of 0.2 m from the plate. Frequency-domain magnetic fields along a path 0.2 m above the plate are calculated with both methods. Fig. 7(b) shows the magnetic fields under three different frequencies. It is found again that the matching is very good, with an average error smaller than 2%. Simulations were performed on a PC with i7-4749 CPU @3.6GHz and 16GB. In the simulation with the proposed method, each of three plates are divided into 20 x 20 cells. The computation time and memory space was 29 sec. and 0.68 G with the proposed method, and 1 hour 29 min. 47 sec. and 9.27GB with the FEM method.

IV. Lightning Transients in a Building

The proposed method is now applied to evaluate impulse magnetic fields and induced voltages within a building in the 1st negative lightning return stroke of 100 kA and 1/200 μs. Fig. 1 illustrates the configuration of a 4-story building under investigation. The building is represented with a wire structure with an interval of 5 m in the *x* and *y* directions, and a vertical interval of 4 m. The grid wire has a diameter of 10 mm, and a conductivity of $5x10^6$ S/m. There is a 4-side metal shield on 3/F with the thickness of 2 mm and conductivity of $3.7x10^7$ S/m. The plate structure is bonded to the wire grid.

A power supply circuit with line (L), neutral (N) and protective earth (PE) conductors run on 3/F, as illustrated in Fig. 1. The spacing between adjacent conductors is 0.1m. PE is bonded to the structure at its two ends.

There are two cases of a lightning strike to the building. In the 1st case, the building structure serves as the down conductors of the LPS. The lightning current injected at the corner of the structure is discharged to the ground via the wire-plate structure. In the 2nd case, an insulated down conductor is provided to discharge the lightning current. The building structure is subject to induced lightning currents. The ground termination of the LPS is made with buried conductors. For simplicity, a grounding electrode is provided at each joint on the ground, and is represented with a serial connected R and L circuit with R=10 ohm and L=10 μH.

Lightning impulse magnetic fields are calculated at the center of the volume within the shield. Fig. 8 shows the results obtained with and without the shield. It is found that the magnetic field at the center drops when the shield is present. In the 1st case, the change of the impulse magnetic field is primarily due to the redistribution of the lightning current, not to the shielding effect. In 2nd case, induced currents are generated in the wire-plate structure. The impulse magnetic field is reduced significantly.

Lightning transient voltages between L and N is also evaluated in these two cases under the lightning stroke. Fig. 9 shows the transient voltages on the line. It is found that the voltage is significantly high when the shield is not present, and can reach 35kV in the direct lightning strike to the building. The transient voltage, however, is significantly small when the metal shield is present. In the lightning strike to the IDC, it is less than 5kV. Although these transient voltages have large peak values, the energy is not that significant because of its short duration. Nevertheless, for sensitive equipment connected to the circuit, surge protective devices need to be provided at the line end to suppress the substantial transient voltage along the circuit.

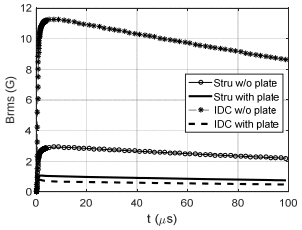

Fig 8. Lightning impulse magnetic fields in two cases.

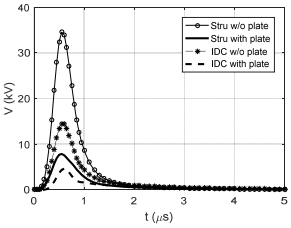

Fig. 9 Transient voltages in the circuit in two cases.

V. Conclusions

An efficient PEEC method was presented for modeling of wire-plate structures and simulation of impulse EM transients. This method was validated experimentally and numerically, and was applied to evaluate lightning transients in a 4-story building. The simulation with this method is much more efficient than the FEM method.

Acknowledgment

The work was supported by grants from the Research Grants Council of HKSAR (Project No. 15203815E and 15210018E).

References

[1] A. Orlandi, “Lightning induced transient voltages in presence of complex structures and nonlinear loads,” IEEE Trans. on EMC, vol. 38, no 2, pp. 150-155, 1996.

[2] Binghao Li, Yaping Du and Mingli Chen, “An FDTD thin wire model for lossy wire structures with non-circular cross section,” IEEE Trans. on PWRD, vol. 33, no. 6, pp. 3055 – 3064, 2018

[3] K. Sheshyekani and M. Akbari, “Evaluation of lightning-induced voltages on multiconductor overhead lines located above a lossy dispersive ground,” IEEE Trans. on EMC, vol. 29, no. 2, pp. 409, 2014

[4] L. Hasselgren and J. Luomi, “Geometrical aspects of magnetic shielding at extremely low frequencies,” IEEE Trans. on EMC, vol. 37, no. 3, pp. 409–420, Aug. 1995

[5] Y. Du and J. Burnett, “ELF shielding performance of metallic enclosure for heavy-current conductors,” IEE Proc. – Gener. Transm. Distrib. vol. 146, no. 3, pp. 223-228, May 1999

[6] A. Canova, G. Gruosso, and M. Repetto, “Integral methods for analysis and design of low-frequency conductive shields,” IEEE Trans. on Magn. vol. 39, no. 4, pp. 2009–2017, Jul. 2003

[7] D. Romano and G. Antonini, “Augmented quasi-static partial element, equivalent circuit models for transient analysis of lossy and dispersive magnetic materials,” IEEE Trans. on Magn., vol. 52 no. 5, pp.1-11, 2016

[8] D. Romano, G. Antonini, A. E. Ruehli, "Time domain PEEC solver including non-linear magnetic materials", IEEE Trans. on Magn., vol. 52, no. 9, 7004911, 2016

[9] Y. Du, Q. B. Zhou and X. H Wang, “Equivalent circuit approach for evaluating low-frequency magnetic fields in the presence of non-ferromagnetic plates,” IEEE Trans. Magn., vol. 45, no. 3, pp. 960–963, Feb. 2009

[10] Nenghong Xia and Y. Du, “An efficient modeling method for 3-D magnetic plates in magnetic shielding,” IEEE Trans. on EMC, vol 56, no. 3, pp. 608-614, 2014

[11] G. Antonini, D. Romano, “Quasi-static partial element equivalent circuit models of linear magnetic materials”, IEEE Trans. on Magn., vol. 51, no. 7, 7003911, 2015

[12] Y. Du, Hongcai Chen and Mingli Chen, “Analysis of transient magnetic shielding made by conductive plates with a PEEC method,” IEEE Trans. on Magn.,vol. 53, no. 6 , 6300404, 2017

[13] B. Gustavsen, "Fast passivity enforcement for pole-residue models by perturbation of residue matrix eigenvalues," IEEE Trans. on PWRD, vol. 23, 2008, pp. 2278-2285.